Theses and Dissertations   1. Thesis and Dissertation Collection, all items

1965

Modeling assumptions for the disposition of solar radiation in an atmosphere with a low overcast.

Bell, James H.

Monterey, California. Naval Postgraduate School

http://hdl.handle.net/10945/24771

MODELING ASSUMPTIONS FOR THE DISPOSITION
OF SOLAR RADIATION IN AN ATMOSPHERE
WITH A LOW OVERCAST

JAMES H. BELL

MODELING ASSUMPTIONS

FOR THE

DISPOSITION OF SOLAR RADIATION

IN AN

ATMOSPHERE WITH A LOW OVERCAST

* * * * * *

James H. Bell

MODELING ASSUMPTIONS FOR THE DISPOSITION OF

SOLAR RADIATION IN AN ATMOSPHERE WITH

A LOW OVERCAST

by

James H. Bell

Lieutenant, United States Navy Reserve

Submitted in partial fulfillment of
the requirements for the degree of

MASTER OF SCIENCE

IN

METEOROLOGY

United States Naval Postgraduate School
Monterey, California

1965

MODELING ASSUMPTIONS FOR THE DISPOSITION

OF

SOLAR RADIATION IN AN ATMOSPHERE WITH

A LOW OVERCAST

by

James H. Bell

This work is accepted as fulfilling

the thesis requirements for the degree of

MASTER OF SCIENCE

IN

METEOROLOGY

from the

United States Naval Postgraduate School

ABSTRACT

A model is presented for the depletion of incoming solar insolation by an atmosphere with a stratus overcast. In the clear air above the cloud, the depletion has been accounted for by a scattering-absorption model due primarily to London [10]. Within the cloud, a spectrally averaged absorption coefficient for liquid water drops is devised. The effect of this absorption coefficient is to bring about abnormally high values of absorption. These absorption values are then reduced to account for scattering, similar to a non-absorbing scattering theory advanced by Fritz [4]. Tests of the solar-depletion model were made by comparison with pyrheliometer data recorded under stratus overcast conditions at Pacific Grove, California, during the summer of 1964.

TABLE OF CONTENTS

LIST OF TABLES

LIST OF ILLUSTRATIONS

LIST OF ABBREVIATIONS AND SYMBOLS

A	absorptivity
A_b	absorptivity within the cloud
A_c	cloud albedo
A_f	Fritz'cloud albedo
A_{wv}	absorptivity of water vapor
D	diffusivity
g	acceleration of gravity
h	cloud thickness
I_{cb}	insolation at cloud base
I_{ct}	insolation at cloud top
I_o	effective insolation at top of atmosphere
I_o'	effective insolation at top of atmosphere without infrared correction
$I_{o\lambda}$	initial intensity of monochromatic radiation
I_λ	final intensity of monochromatic radiation
K_1, K_2	constants in Davis' equation for water vapor
K_s	scattering area coefficient
$\bar{k}$	average liquid water absorption coefficient
$k_{\lambda\omega}$	monochromatic liquid water absorption coefficient
ℓ	thickness of pure water
L	mean free path of light
Ly	Langley $= cal/cm^2$
m	optical air mass $\cong sec z$
n_i	number of droplets of radius r_i per unit volume
P_b	pressure at cloud base
P_c	pressure at cloud top
P_i	average pressure in an atmospheric layer

P_o	Standard surface pressure $= 1013$ mb
P_t	pressure at cloud top
Q_i	average mixing ratio in an atmospheric layer
r	radius of droplet
R	sun-earth distance
R_M	mean sun-earth distance
r_{xy}	linear correlation coefficient between X and Y
S	fractional depletion by scattering
S_A	diffusivity due to dry-air scattering
S_D	diffusivity due to dust scattering
S_{wv}	diffusivity due to water vapor scattering
T	transmissivity
u_b	optical depth at cloud base
u_s	optical depth at surface
u_t	optical depth at cloud top
u'_b	corrected optical depth at cloud base
u'_c	corrected optical depth at cloud top
u'_s	corrected optical depth at surface
W	length of path through air containing water drops
x_i	observed value of surface insolation
y_i	computed value of surface insolation
Z	zenith angle
ΔP_i	pressure thickness of an atmospheric layer
Δu_i	increment of optical depth in an atmospheric layer
$\Delta u'_i$	increment of corrected optical depth in an atmospheric layer
λ	wave length

viii

ACKNOWLEDGEMENT

Appreciation is due to Professor Frank L. Martin, of the Department
of Meteorology and Oceanography, for the guidance and advice which was
provided during the preparation of this thesis.

1. Introduction

Solar radiation is depleted by a number of scattering and absorption processes in its traverse of the earth's atmosphere. These processes have been handled in a variety of models some of which treat the depletion in a definite order and others of which allow the various depleting agents to act simultaneously.

The greatest variation occurs in the manner in which depletion by clouds is treated. Fritz [4] presents a theory treating the case of scattering by non-absorbing water droplets within the cloud. He indicates that the upper limit to this scattering or albedo increases toward unity with increasing cloud thickness. Neiburger [11] estimates a mean cloud absorptivity of seven per cent with little deviation relative to this value in the case of California stratus. His cloud albedo appears to approach a definite upper limit of 80% with increasing cloud thickness, thus indicating scattering as a more important depletive process than absorption. Neiburger's observations of transmissivity were consistently greater than those of his estimated absorptivities.

Bullrich et al [1] of the Johannes Gutenberg University, have found that absorption may exert a marked reduction on scattering in the case of absorbing aerosols (such as water drops). Their investigation showed that as the absorption coefficient increases, the scattering coefficient decreases in a turbid atmosphere.

In this investigation depletion in cloud free layers primarily follows London's [10] model. Within the cloud layer, absorption is taken as the initial approximation to be the first depletive process. Secondarily, the scattering depletion is removed from the overestimate

1

of absorption in a manner suggested by Fritz' theory. The model pro-
posed here gives good agreement with pyrheliometric observations under
the overcast, and values of cloud albedo in reasonable agreement with
observed values proposed by Fritz [4] and Neiburger [11] .

The model has been used to obtain mean estimates of cloud albedo
and planetary albedo over a black-soil area in Pacific Grove, California.

2. Preliminary procedure

During the period from May to September 1964, Cole and Brown [2] obtained data from a continuous recording pyrheliometer which they mounted at Point Pinos in Pacific Grove, California. In their paper they list cloud amounts as well as the cloud tops and bases as reported by airline pilots over this point. Both reporting times and cloud data were communicated accurately to the Monterey airport control tower by the cooperating pilots, and these data were systematically collected, along with pyrheliometric traces, in the Cole and Brown paper.

In this study, a random set of 22 overcast cases with all the other reports available, including a recent radiosonde, was made at reporting times ranging between 0730 to 1030 PST.

Since upper air soundings are not taken at Monterey, the 1200 GCT (0400 PST) Oakland sounding was plotted for each of the 22 days selected. The cloud layer was marked on these soundings and the optical depth ($\Delta_i u$) computed for successive sounding intervals $i=1,\dotsc,n$ from the top to the bottom of the sounding by the formula:

$$\Delta_i u = \left(1000/g\right) Q_i \Delta P_i \tag{1}$$

The integrated optical depth was obtained by summing these intervals in three steps: (1) 200 mb to cloud top (2) cloud top to cloud base (3) cloud base to surface. The _corrected_ optical depth of a thin layer of central pressure P_i is obtained by:

$$\Delta_i u' = 1000/g \left(P_i/P_o\right) Q_i \Delta P_i \tag{2}$$

3

Here the factor (P_i/P_o) represents the multiplicative correction factor to $\triangle_i u$ in expressing the pressure broadening effect of air on water-vapor absorption. The integrated corrected optical depth is then summed in a similar manner to that employed for optical depth.

The solar constant, 2.00 ly(min)$^{-1}$, was then corrected for various factors. In accordance with Johnson's [8] analysis, .095 ly(min)$^{-1}$ was subtracted for ultra-violet absorption above the troposphere and .066ly(min)$^{-1}$ was subtracted for the infrared correction due to water vapor absorption in wave-lengths greater than 2.4 microns. The resultant value 1.839 ly(min)$^{-1}$ is multiplied by $(R_M/R)^2$ to compensate for sun-earth distances different from the mean $(R_M = 92.6 \times 10^6$ mi).

The zenith angle (Z) for each date-time case was obtained from the Smithsonian Meteorological Tables [9] . The time was taken as the exact reporting time of the airline pilot. From the tables the optical air mass, m = sec.Z, was readily computible. As a further correction, the reduced solar radiation was multiplied by cosZ, giving the "effective" starting insolation(I_o):

$$I_o = 1.839 \left(R_M/R \right)^2 \cos Z \qquad (3)$$

The insolation at the top of the atmosphere is then depleted as described in the following sections.

3. Depletion above the cloud layer

The depletion from the top of the atmosphere to the top of the overcast was essentially computed after London [10] . The final expression for the insolation at the cloud top is of the form:

$$I_{ct} = I_o \left\{ 1 - A_{wv} - \tfrac{1}{2} S_A - \tfrac{1}{2} S_D - \tfrac{1}{4} S_{wv} \right.$$
$$\left. - \tfrac{3}{4} S_{wv} \left[K_1 \left(1.5 \, m \, u'_c \right)^{K_2} \right] \right\} \tag{4}$$

with the symbols defined as follows:

I_{ct}	insolation at cloud top
I_o	corrected insolation at top of atmosphere
A_{wv}	absorptivity due to water vapor
S_D	diffusivity due to dust scattering
S_A	diffusivity due to Rayleigh scattering by dry air
S_{wv}	diffusivity due to water vapor scattering
m	optical air mass $= secZ$
K_1, K_2	constants discussed below
u'_c	corrected optical depth at cloud top

The values for A_{wv}, S_{wv}, and S_A were obtained, for simplicity, from empirical curves (fig. 1) developed by Houghton [7] . These curves yield values of transmissivity (T) accurate to two significant digits from which diffusivity (D) or absorptivity (A) is obtained by the equations:

$$D = 1 - T \qquad\qquad A = 1 - T$$

Transmissivities after water-vapor scattering and absorption are functions of optical depth (u) and optical air mass (m) reduced by the factor P_c/P_o after Houghton [7] . The argument in fig. 1 is thus $(m u P_c)/P_o$.

Transmissivity due to Rayleigh scattering is a function only of optical air mass and therefore the entering argument is $(mP_c)/P_0$.

The transmissivity after dust scattering has been taken following both Houghton [7] and London [10]:

$$T_D = (.95)^{m\,P_c/P_0}$$

In equation (4) various coefficients (such as $\frac{1}{2}$ or $\frac{1}{4}$) of the diffusivity or absorptivity are taken as the net depletion depending on the particular scattering or absorbing process involved. The coefficients are based primarily on London's model [10].

Rayleigh scattering by dry air is considered isotropic and therefore one-half of S_A acts to deplete the insolation. Similarly one-half of S_D is taken as depletion, the depletion being caused equally by back-scattering and absorption.

The factor $\frac{1}{4}$ multiplying S_{WV} is also modeled after London, with the implication that the one-fourth of the scattering depletion by water vapor is scattered to space, while three-fourths is scattered down. The reason for this asymmetry is not clear, although, the most plausible reason in the relatively dry Pacific summer air may be associated with a positive correlation between the dust and water vapor contents of the air. However, it should be noted that water vapor absorption has been removed from the 3/4 S_D, whereas the full $\frac{1}{4} S_D$ is considered to be part of the planetary albedo.

In equation (4) the other factor in brackets multiplying 3/4 S_{WV} represents the fraction of S_{WV} actually absorbed by water vapor. This absorption factor has been given by

$$K_1 (1.5\, m u'_c)^{K_2}$$

6

after Davis $[3]$. Davis cites the values of the constants K_1, K_2 as $K_1 = 0.100$, $K_2 = 0.300$ for cloud tops below the 500 mb level, and $K_1 = 0.4$, $K_2 = 0.084$ for cloud tops above the 500 mb level. The factor 1.5 was applied to correct the direct-beam path in order to account for the greater path length involved in scattering, especially when multiple scatterings are considered. Implicitly, this same factor, 1.5, has been "built into" S_A and S_{wv}, since Houghton's curves (fig. 1) are modifications of scattering observed by the Smithsonian Institute group.

4. Depletion within the cloud layer

The insolation at the cloud base (I_{cb}) has been computed in accordance with the formula

$$I_{cb} = I_{ct} \left\{ 1 - (1 - e^{-\bar{K} \, 1.62 \, m\ell}) - A_{wv} \right.$$
$$\left. - S_A - \tfrac{1}{4} S_{wv} - \tfrac{3}{4} S_{wv} K_1 [1.62 \, m(u'_b - u'_t)]^{K_2} \right\} \qquad (5)$$

With the exception of the wavy-underlined term in parentheses, the expressions are exactly as identified in the preceding section.

The values of A_{wv}, S_A, and S_{wv} are obtained from Fig. 1 as before, except the entering argument for the water-vapor terms is 1.62 $(u_b P_b - u_t P_t)/P_o$. For the Rayleigh scattering term $1.62m(P_b - P_t)/P_o$ is used, where "b" and "t" subscripts refer to the base and top of the cloud, respectively.

The factor 1.62 is applied either directly or indirectly to the path length in all terms in the cloud. This factor was suggested by Houghton [7] to account for the fact that diffused sky light emerges from the cloud base. It expresses the greater scattering probability within (and below) the cloud than above it, where the corresponding factor was 1.5.

The depletion by dust diffusivity is ignored as it is more than compensated for by liquid-water scattering and absorption as described below. The major change within the cloud layer is due to the effect of absorption by liquid water.

Recall that for water-vapor scattering and absorption, Houghton's empirical graphs [7] , applicable over the entire solar spectrum, were used. A similar approach was considered desirable in dealing with liquid water absorption.

8

For values of $k_{\lambda w}$ listed in the Smithsonian Meteorological tables [9, p.447] for liquid water, one may write the monochromatic transmissivity (T_λ) of liquid water in the form

$$T_\lambda = \frac{I_\lambda}{I_{o\lambda}} = e^{-k_{\lambda w}\ell} \tag{6}$$

$I_{o\lambda}$ initial intensity of a parallel beam of monochromatic radiation

I_λ intensity after passing through water

ℓ thickness of liquid-water absorbing path

$k_{\lambda w}$ absorption coefficient

Table 156 of the Smithsonian Meteorological Tables [9] lists absorption coefficients for comparatively small wave-length intervals from .310 to 2.650 microns. One way of obtaining an average absorption coefficient, which would act uniformly over the entire solar spectrum, is to average all the $k_{\lambda w}$ with respect to λ from .310 to 2.44 microns. Each $k_{\lambda w}$ is weighted by the length of the wavelength interval for which it is listed. The mean value computed by this method, denoted $\overline{k}$, becomes

$$\overline{k} = 16.89 \ cm^{-1}$$

This value was taken to be 17.0 cm^{-1} for computational purposes.

The value of ℓ, the thickness of the water-absorbing path in centimeters per cm^2 of beam was found by using the known cloud thickness and arbitrarily assuming a constant water density of 0.5 g/m^3. The actual thickness of water traversed by the insolation was found by multiplying ℓ by the recurring factor 1.62m. The expression for

9

depletion by liquid-water absorption is thus modified to:

$$1 - e^{-\bar{k}(1.62\, ml)}$$

The value for depletion by this term is naturally unrealistically high as this computation of an average absorption coefficient spreads the effects of strong absorption in the infrared into the visible region where the Smithsonian Tables [9] list small coefficients. However, in the actual computation with the average $\bar{k}$, the liquid-water absorptivities reduce the entering insolation at cloud tops by 40 to 70 %. Hence, these absorptivities have been reduced by the upward-scattering loss from the cloud particles while not affecting the total depletion.

5. Discussion of the liquid water absorption term

As just noted, the values obtained for liquid water absorption are overestimated. However, this procedure gives values closely approximating the total depletion by the cloud. As already noted, this overestimated absorption must be reduced by upward scattering.

Houghton and Chalker [6] developed an expression for the transmission after scattering of radiation by water droplets in air:

$$T = I/I_o = e^{-(\Sigma \pi n_i r_i^2 K_s)W} \tag{7}$$

I_o initial intensity of parallel beam

I intensity after passing through water droplets

W path length in centimeters through air containing water droplets

n_i number of droplets of radius r_i in a unit volume

K_s scattering-area coefficient

In the Houghton-Chalker *approach,* the Mie scattering theory was used. Here the scattering coefficient (K_s) is a function of the parameter:

$$\alpha = 2\pi r / \lambda$$

r radius of the droplet

λ wavelength of incident radiation

The scattering coefficient is less selective with respect to wavelength as the ratio of particle diameter to wavelength becomes large (see Fig. 2). Equation (7) could then be summed for all water droplet sizes present, and would be averaged over the spectral interval involved if the incident beam were not monochromatic.

11
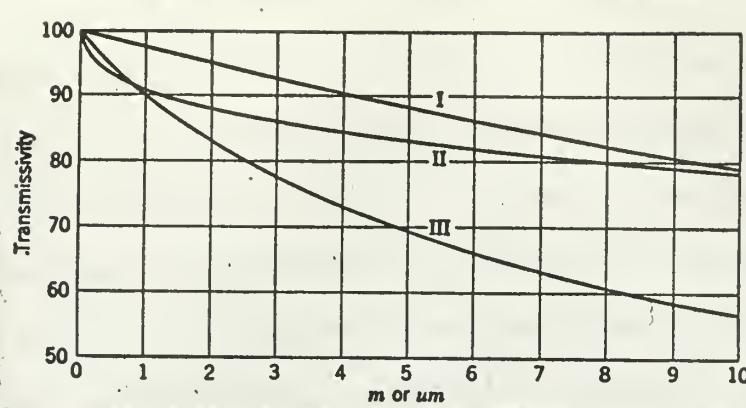
Fig. 1. Atmospheric transmission curves. (after Houghton) I: transmission
due to water-vapor scattering II: transmission due to water-vapor
absorption III: transmission due to scattering by dry, dust free air.
For curves I and II, abscissa is the product mu; for curve III, abscissa
is m.
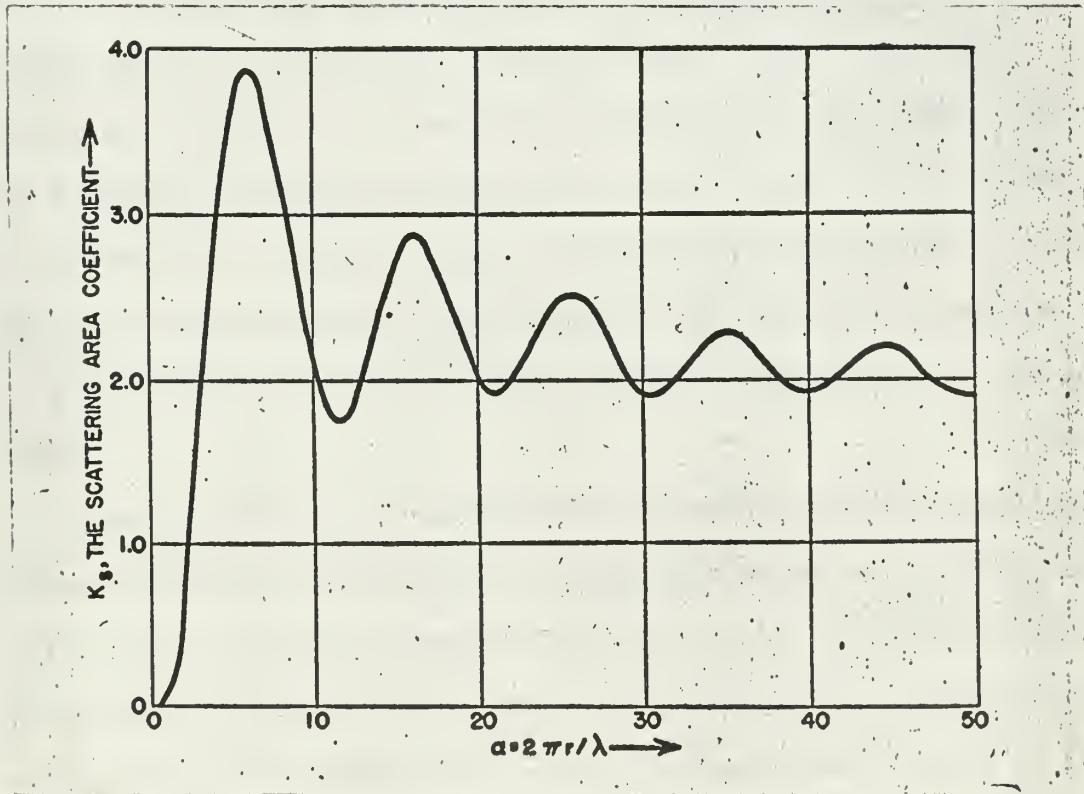
Fig. 2. Scattering area coefficients for water drops in air as a
function of droplet radius (r) and wavelength (λ). [After Houghton
and Chalker (6).]

For values of $\alpha \geq 6.0$, there is considerable scattering
associated with a series of maximum and minimum values of K_s. Since
α is a function of r and λ , it can be seen that a cloud having
a varied spectrum of drop sizes will have drops of the appropriate diam-
eter to give fairly uniform amounts of scattering over a wide range of
wavelengths. In other words, scattering is essentially diffused over
all wavelengths of the solar spectrum within the cloud droplet medium.
Samplings of drop sizes in stratus clouds by Neiburger [11] indicated
such a diversity of drop sizes.

Hewson's [5] investigation tended to show that reflection from
clouds was reasonably independent of wavelength, throughout the visible
region and up to 1.4 microns in the infrared. Thus, since the
scattered extinction is essentially independent of wavelength, and
our synthetic absorption-extinction has been forced to be independent
of wavelength, a realistic portion of the overestimate of this diffuse-
wavelength absorption can be considered to account for diffuse scattering
by water droplets, which will then also be diffuse relative to wave-
length.

Consequently, we are approaching an albedo first as a result of
enhanced absorption (temporarily neglecting scattering). The approach
is analogous, but with an opposite starting point, to that of Fritz [4]
who develops an albedo based upon the consideration of scattering with
no absorption. Presumably, his values of albedo would have to be
reduced if liquid absorption were proceeding simultaneously, a result
strongly emphasized by Bullrich et al [1].

6. Cloud albedo

The value for cloud albedo is obtained from the equation:

$$A_c = A_F \left(1 - e^{-\bar{k} \, 1.62 \, \ell m}\right) + \frac{1}{2} S_A + \frac{1}{4} S_{wv}$$

(8)

A_c cloud albedo

A_F cloud albedo as derived by Fritz

A deficiency of the Houghton-Chalker [6] scattering theory is that with constant droplet size it leads to abnormally large forward scatter. Fritz [4] attempts to correct this deficiency by intro-ducing random orientation of second and higher order scatterings. Thus, Fritz obtains values in fairly close agreement with cloud albedos measured by Neiburger [11] for deep cloud layers. However, Neiburger's cloud absorptivities appear to be too small in light of the Mie theory.

Fritz obtains cloud albedo as an increasing function of h/L and zenith angle. Here h is the cloud thickness and L is the mean free path of a scattering occurrence given by Fritz as

$$L = 1 / \left(\sum N_i \, \pi \, r_i^2 \right)$$

Here N_i is the number of drops of radius r_i per cubic centimeter. The summation is taken over all droplet sizes present. For this investigation an extrapolated value of h/L was obtained using a constant water density of $0.5 g/m^3$, and a cloud thickness of 1000 feet. The extrapolation based upon observed h and an assumed droplet density equal to that of Neiburger's is shown in table 1.

Table 1.	Some values of h/L and associated water densities			
	(a)	(b)	(c)	(d)
Average water density (g/m^3)	0.19	0.30	0.34	0.50
h/L	4.2	6.8	7.5	10.9

(a), (b), (c) are selected cases from Neiburger's [11] study. Case (d) is extrapolated for use in this study.

As shown above, the extrapolated value of h/L thus obtained was

$$h/L = 10.9$$

For cloud thicknesses different than 1000 feet, values are obtained from the formula

$$h/L = h/1000 \ (10.9)$$

that is, L has been considered to be constant throughout the data-sample of this study. With the value of h/L thus obtained, and the zenith angle known, the albedo is obtained from fig. 3 after Fritz [4] In this figure, Fritz considered no cloud absorption, so his values of cloud albedo are considered too large. For this reason, the value of the cloud albedo is applied only to the depletion originally designated as due to extinction by cloud water and not to the total inso-lation incident at the cloud top. In addition, equation (8) adds to this component the minor components due to upward scattering by dry air and water vapor to obtain the final value for cloud albedo. These minor additions are handled similarly to the procedures for upward scattering employed in section 3.

It should be noted that the cloud albedo is defined as the reflectivity which would be observed just above the cloud, and not that which would be observed at the top of the atmosphere.
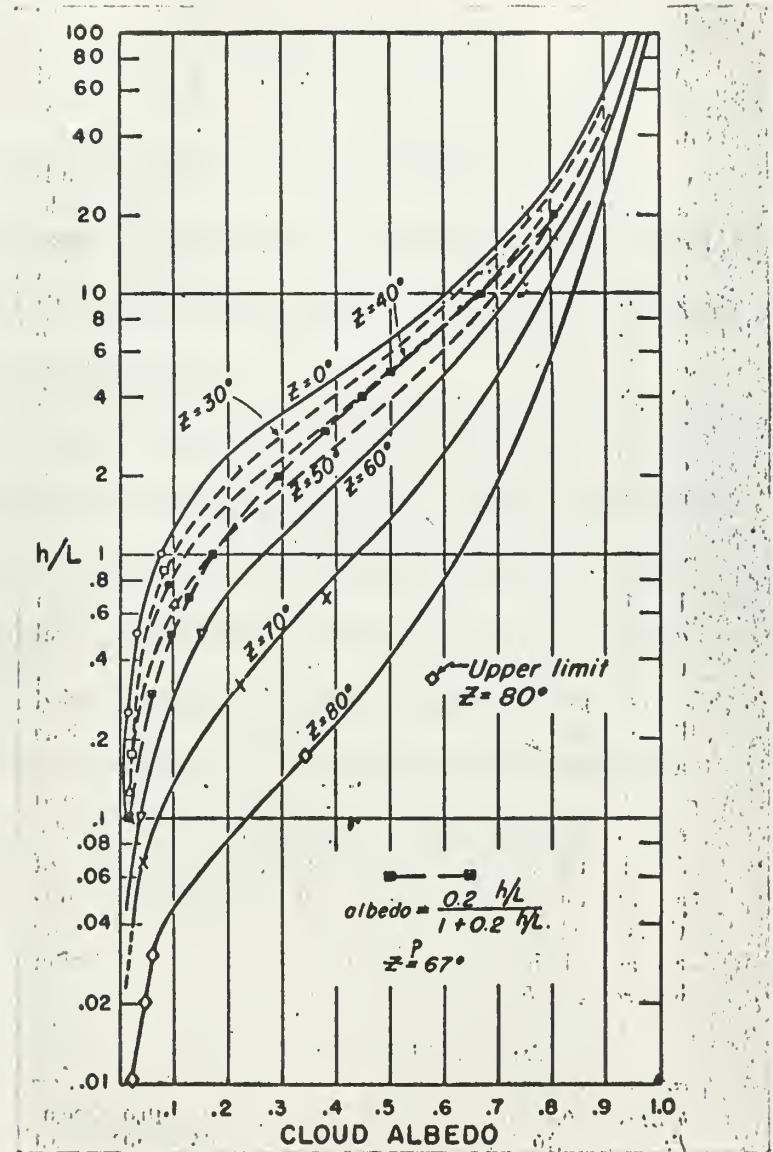
Fig. 3. Cloud albedo as function of h/L for various values
of zenith angle. Underlying surface albedo and sky
radiation zero. [After Fritz (4).]

7. Depletion below the cloud base

The formula for insolation at the earth's surface (I_s) may be written

$$I_s = I_{cb} \left\{ 1 - A_{wv} - \tfrac{1}{4} S_{wv} - \tfrac{1}{2} S_A - \tfrac{1}{2} S_D \right.$$
$$\left. - \tfrac{3}{4} S_{wv} K_1 \left[1.62 \, m \, (u'_s - u'_b) \right]^{K_2} \right\} \tag{10}$$

The factor 1.62 is applied to m in all cases to allow for the diffuse nature of the radiation below the clouds. All terms are as defined in previous sections.

All water vapor terms are obtained from Fig. 1, using the independent variable $1.62m(u_s P_s - u_b P_b)/P_o$, while the Rayleigh scattering term is obtained with $1.62m(P_s - P_b)/P_o$ as the independent variable for entering the graph. Here "b" and "s" subscripts refer to the cloud base and earth's surface, respectively.

For dust transmissivity (T) the expression used is:

$$T = (.95)^{1.62 \, m \left(\frac{P_s - P_b}{P_o} \right)}$$

17

8. Results

The results of the computations involved in the model are tabulated in table 4. The values given for the various depleting agents must be multiplied by the value of insolation incident at the top of the layer in which they operate to obtain a value of depletion in $ly/(min)^{-1}$.

As a check on the accuracy of the model, a correlation analysis between the observed and the model-computed values (x and y, respectively) of surface insolation was performed. Graphical results, depicted in Fig. 4, indicate that a high positive value of the linear correlation is to be expected. The simple correlation coefficient between paired values of computed and observed surface insolation was computed. The value of the resulting correlation coefficient was

$$r_{xy} = 0.916$$

with a linear regression equation

$$y - 0.3618 = 1.132 \, (x - 0.3315)$$

As a test of the significance of this correlation coefficient, the F-test was applied in the form suggested by Panofsky and Brier[12]

$$F = \frac{r_{xy}^2}{1 - r_{xy}^2} \, (N-2)$$

where N is the number of independent data-pairs (x_i, y_i).

With $r_{xy} = 0.916$, F has the value

$$F = 104.22$$
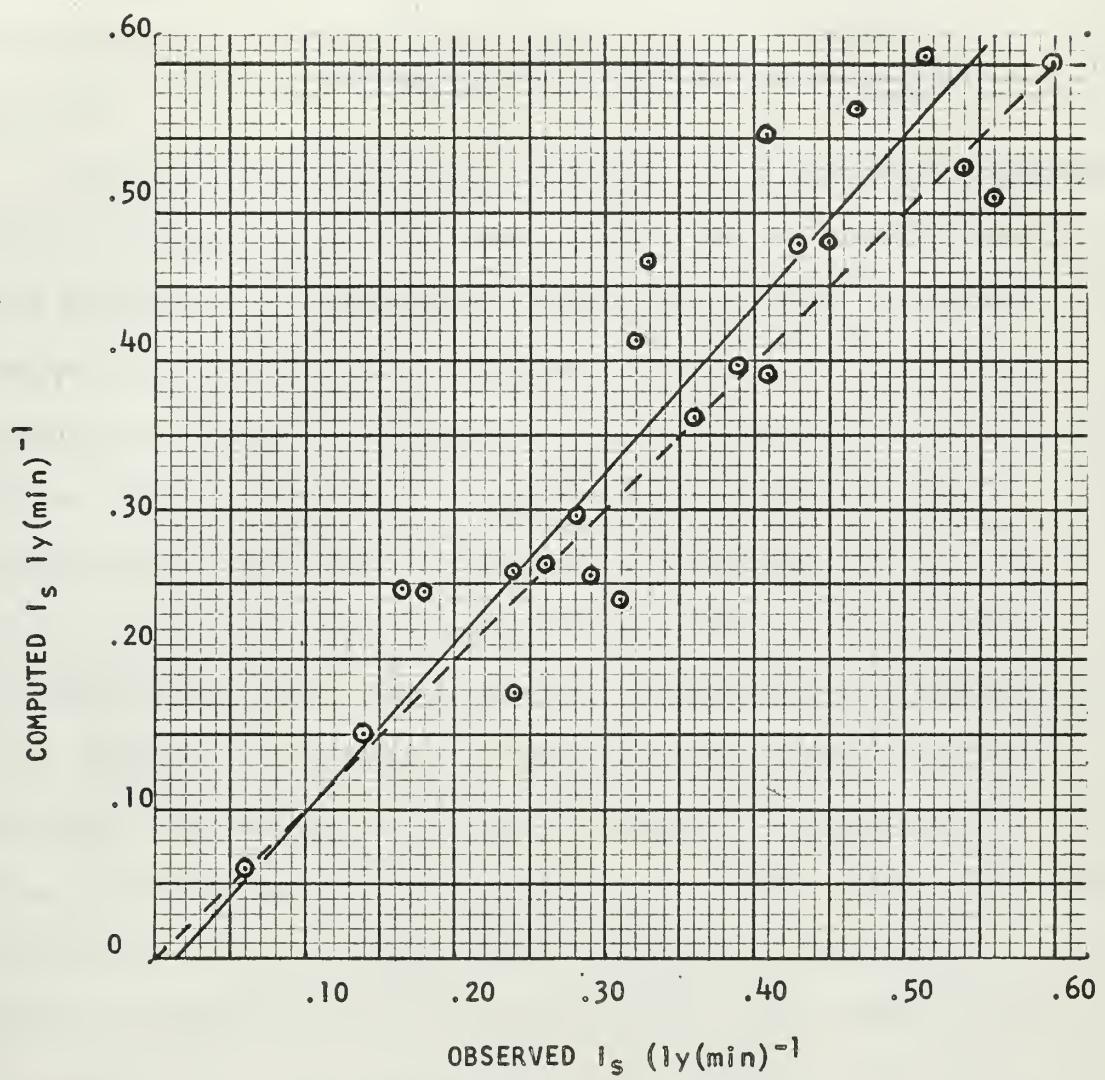
Fig. 4. Scatter diagram of computed insolation against observed, with stratus overcast at Pacific Grove, California.

_____ = best-fitting regression line

----------- = ideal model

Statistical tables of F values with 1 and 20 degrees of freedom indicate that the linear correlation is significantly different from chance at a confidence level well in excess of 99.9% probability.

From table 4 (see Appendix), computed mean values of the undepleted solar insolation and its subsequent disposition are computed based upon the averages of the present sample. The computations extend progessively from the top of the atmosphere to the surface and are summarized in table 2. Consequently, it was necessary to add back the infrared correction, converted to an insolation, thus modifying the "starting" insolation (I_o) of equation 3 to I_o', since this is energy absorbed by atmospheric water vapor. The infrared correction, converted to an insolation, represents a mean addition of 0.044 $ly(min)^{-1}$, to the mean of I_o computed from table 4. Of this additional insolation, two-thirds is assumed to be absorbed above the cloud, and the remaining one-third within the cloud. This subdivision is somewhat arbitrary; however, some allowance has been made for the pressure broadening and also scattering. The latter tends to lower the level at which absorption takes place. Because of the nature of the surface (dark soil) at the pyrheliometer installation, the surface albedo has been taken to be zero.

In table 2, the mean cumulative fractions of absorbed and scattered energy as well as of cloud albedo are computed based upon averages of appropriate columns in table 4. One may also estimate the planetary albedo as viewed from space. This includes the full contribution of back-scatter under column 1 of table 2 (since this was a net result after the action of all other depletive processes)

20

Table 2. The average disposition of the solar insolation based upon the model.

undepleted insolation $I_o' = 1.278$ ly(min)$^{-1}$

Depleting agents	I — Above cloud absorption	I — Above cloud back-scatter	II — Within cloud absorption I_{ct} entering = 0.926 ly(min)$^{-1}$	II — Within cloud back scatter	III — Below cloud absorption I_{cb} entering = 0.347 ly(min)$^{-1}$	III — Below cloud scatter
(a) liquid water	—	—	13.9%	36.31%	—	0.05%
(b) dry air	—	6.59%	—	0.56	—	0.5
(c) water vapor	17.45%	1.49	8.4	0.53	7.7%	—
(d) dust	0.57	0.57	—	insignificant	see foot-note	0.1
(e) water-vapor absorption of water-vapor scattering	0.65	—	0.11	—	—	0.5
TOTALS	18.7%	8.65%	22.4%	37.30%	8.2%	1.1%

Enter Col. II with Ict = 0.926 ly(min)$^{-1}$

Enter Col. III with Icb = 0.374 ly(min)$^{-1}$ (see footnote) Final I_s = 0.347 ly(min)$^{-1}$

A = 37.3
S = 35.6

Cumulative absorption (%), based on $I_o' = 1.278$ ly(min)$^{-1}$
Cumulative back scatter (%), based on $I_o' = 1.278$ ly(min)$^{-1}$
Mean cloud albedo (%), based on cloud top insolation: 37.3
Mean planetary albedo (relative to I_o') as observable ≅ 8.65 + 21.4 ≅ 30.1
at the top of the atmosphere

[1]Note that the "scatter" of column III is assumed, in view of our model characteristics, to be absorbed (one-third) and the remainder ultimately forward scattered (two-thirds). Also the surface albedo was essentially zero.

together with the cloud albedo reduced by the mean absorptivity of the space above the cloud. In connection with the latter, no allowance is made here for downward scattering of the beam reflected from the cloud since it is felt that ample allowance was made for this process in those computations made "above the cloud" in table 4. However, the upward reflected beam is subject to absorption in much the same manner as was the downward insolation. Since the infrared – corrected wavelengths have been removed, the mean transmissivity to be applied to the cloud reflection is

$$\left[1 - \frac{(18.7 - 2.9)}{100} \right] = 0.842$$

and the cloud energy thus transmitted to space is 21.4%. The subtraction 18.7 - 2.9 indicates that the infrared – correction energy has been deleted. Thus an estimate of the cloud albedo which reaches space is $0.842\ A_c$.

9. Further statistical considerations of the computational model

Two regression analyses were made in this study to test the reality
of the computational model. The first, correlated computed against
observed values of the surface insolation and led to surprisingly good
results.

In order to test the theoretical behavior of the cloud albedo, a
linear multiple regression of computed A_c as a function of the indepen-
dent variables cloud depth (h) and secZ was conducted. It is realized
that both independent variables have been built into A_c (equation 8)
and therefore, there is actual functional dependence upon them. However,
the purpose of this approach is to determine how much each variable
contributes to the computed variation $A_c - \overline{A_c}$ and to estimate the physical
reality of the induced change. The multiple regression is developed
in the convenient form below after Panofsky and Brier [12]

$$\frac{A_c - \overline{A_c}}{\sigma_A} = K_3\, r_{12.3}\, \frac{(h - \overline{h})}{\sigma_h} + K_4\, r_{13.2}\, \frac{(m - \overline{m})}{\sigma_m}$$

(1)   (2)   (3)

where K_3, K_4 are defined as follows:

$$K_3 = \left(\frac{1 - r_{13}^{\,2}}{1 - r_{23}^{\,2}} \right)^{1/2} \qquad K_4 = \left(\frac{1 - r_{12}^{\,2}}{1 - r_{23}^{\,2}} \right)^{1/2}$$

Here numerical labels 1, 2, 3 have been introduced under each term in
the regression equation in order to simplify the notation, and the use
of reference formulas. The results of the CDC computer multiple
regression analysis (based upon BIMD 06) for the 22-case sample are
summarized in table 3.

23

Table 3. Results of the multiple regression analysis.

Sample means			Standard deviations			Simple correlation coefficients		
$\overline{A_c}$	$\overline{h}$	$\overline{m}$	σ_1	σ_2	σ_3	r_{12}	r_{13}	r_{23}
0.3631	1097.73	1.513	0.09698	300.19	0.3380	0.7229	0.548	-0.171

Partial correlation coefficients		Per cent explained variance added
$r_{12.3}$	$r_{13.2}$	$\Delta\sigma_A/\sigma_A$
0.9737	0.9871	By h: 30.03
		By m: 67.35

Per cent variance not explained by regression: 2.62

Multiple regression coefficient $R_{1.23} = 0.9965$

Although A_c depends functionally upon h and m, it is of interest
to see how close a result to linearity this theory gives. The multiple
correlation coefficient $R_{1.23} = 0.9965$, and therefore the final result
is

$$A - 0.3631 = \left(1 - r_{23}^2\right)^{-\frac{1}{2}} (0.09618)$$

$$\left[1.172\left(\frac{h - 1097.73}{300.19}\right) + 1.449\left(\frac{m - 1.513}{0.3380}\right)\right]$$

Thus, within the range of statistical validity of the multiple
regression analysis, the cloud albedo determined by the model was a
linear function of cloud depth (h) and optical air mass. If one
applies the multiple regression equation to a total cloud depth $h-\overline{h} =$
3.0(300.19 ft), of approximately 2000 ft, the albedo is increased from
0.3618 to 0.4819, a rather nominal increase compared to Neiburger's [11]
observations in 2000-foot clouds.

24

The equation used to obtain A_c in the preceding sections was essentially

$$A_c = (I_{ct} A_b) A_F \qquad (11)$$

where A_b = absorptivity within the cloud (over estimated)

A_F = Fritz' determination of cloud albedo

Equation 11 , as written, is in the usual form of the intensity of the direct insolation inside the cloud provided the total scattering fraction $S = A_F$. Furthermore, equation 11 tacitly assumes that absorptivity and upward cloud reflectivity are proceding as independent probability functions. An alternative computation which would lead to higher values of A_c is the following

$$A_c = I_{ct} A_F - I_{ct} k A_b \qquad (12)$$

where $k < 1.0$ is a fraction (to be determined under various conditions) concerning the center of gravity of the penetration depth from which the scattered radiation emerges, as well as the droplet concentration and "size". Thus, for example, Neiburger's [11] drop size determinations show a sharp decrease in mean diameter as the top of the cloud is approached. If the drops near the top are of submicron size, they become very effective scatterers in visible light, while absorbing little solar radiation, since the total water content is small in the top stratum of cloud. This effect appears to be of most probable occurence near noon when insolation at cloud tops is likely to cause evaporation and size reduction of the drops. Of course, the situation will no longer be governed by equation (12) when holes develop in the clouds, since reflection from the sides then adds a bias in the downward direction giving rise to greater surface insolation.

25

Actually an expression like equation (12) *is predicated upon the* generalized Mie theory, which takes account of both scattering and absorption depletion effects. For "thin" clouds of the order of $1000 \overset{+}{-} 300$ ft, the theory developed here seems to give results compatible with those observed both for surface insolation and upward scattering.

BIBLIOGRAPHY

1. Bullrich, K., E. de Bary, K. Danzer, R. Eiden, K. Heger. Research on Optical Radiation Transmission. AF61(052)-595, AFCRL-65-109, Scientific Report 3, Meteorologisch-Geophysikalisches Institut der Johannes Gutenberg-Universitat, January, 1960.

2. Cole, L. I. and D.S. Brown, A Preliminary Correlation of Pyrheliometer Radiation Readings to the Thickness of Stratus at Monterey, California. An unpublished paper, U.S. Naval Postgraduate School, Monterey, California, September, 1964.

3. Davis, P.A. An analysis of the Atmospheric Heat Budget. Journal of the Atmospheric Sciences, v. 20, Jan., 1963: 5-22.

4. Fritz, S. Scattering of Solar Energy by Clouds of "Large Drops". Journal of Meteorology, v. 11, Aug., 1954: 291-300.

5. Hewson, E.W. The Reflection, Absorption, and Transmission of Solar Radiation by Fog and Cloud. Quarterly Journal of the Royal Meteorological Society, v. 69, 1943: 47-62.

6. Houghton, H. G. and W.R. Chalker. The Scattering Cross Section of Water Drops in Air for Visible Light. Journal of the Optical Society of America, v. 39, Nov., 1949: 955-957.

7. Houghton, H. G. On the Annual Heat Balance of the Northern Hemisphere. Journal of Meteorology, v. 11, Feb., 1954: 1-9.

8. Johnson, F. S. The Solar Constant. Journal of Meteorology, v. 11, Dec., 1954: 431-439.

9. List, R. J. (ed.) Smithsonian Meteorological Tables-Sixth Revised Edition. Smithsonian Institution, 1951.

10. London, J. A Study of the Atmospheric Heat Balance. AFCRC-TR-57-287, Final Report, Contract No. AF19(122)-165, College of Engineering Research Division, New York University. July, 1957.

11. Neiburger, M. Reflection, Absorption, and Transmission of Insolation by Stratus Cloud. Journal of Meteorology, v. 6, Apr.,1949: 98-104.

12. Panofsky, H. A. and G. W. Brier, Some Applications of Statistics to Meteorology. The Pennsylvania State University, 1963.

Table 4.   Part 1.   Computations associated with depletion above the cloud.

Date	Z	I_o	$\frac{1}{2}S_D$	A_{wv}	$\frac{1}{2}S_A$	S_{wv}	W.V. absorp.of 3/4 S_{wv}	I_{ct} ly(min)$^{-1}$
18 May	32°19'	1.517	0.028	0.100	0.055	0.008	0.0025	1.224
22 May	38°40'	1.402	0.030	0.105	0.058	0.006	0.0024	1.121
23 May	49°20'	1.168	0.035	0.116	0.065	0.010	0.0040	0.899
30 May	37°59'	1.409	0.030	0.100	0.060	0.006	0.0021	1.131
31 May	36°40'	1.432	0.029	0.105	0.060	0.008	0.0026	1.140
3 Jun	61°30'	0.851	0.049	0.142	0.088	0.019	0.0081	0.591
13 Jun	50°00'	1.145	0.036	0.150	0.068	0.021	0.0093	0.820
26 Jun	52°12'	1.090	0.038	0.130	0.066	0.016	0.0068	0.811
28 Jun	37°42'	1.406	0.029	0.106	0.058	0.006	0.0023	1.122
29 Jun	32°12'	1.504	0.027	0.110	0.052	0.007	0.0025	1.206
5 Jul	39°20'	1.373	0.031	0.123	0.060	0.012	0.0051	1.056
6 Jul	44°50'	1.260	0.033	0.130	0.062	0.016	0.0072	0.947
7 Jul	36°40'	1.426	0.029	0.124	0.060	0.012	0.0049	1.098
18 Jul	57°40'	0.953	0.043	0.160	0.080	0.025	0.0121	0.648
25 Jul	52°20'	1.088	0.038	0.174	0.070	0.031	0.0159	0.730
29 Jul	52°20'	1.091	0.038	0.165	0.072	0.026	0.133	0.747
30 Jul	37°00'	1.426	0.028	0.133	0.055	0.014	0.0058	1.089
8 Aug	63°50'	0.787	0.052	0.165	0.088	0.025	0.0121	0.517
11 Aug	50°59'	1.127	0.036	0.142	0.070	0.019	0.0081	0.817
13 Aug	37°42'	1.418	0.030	0.136	0.058	0.016	0.0069	1.068
14 Aug	41°00'	1.353	0.030	0.122	0.058	0.012	0.0045	1.047
15 Aug	63°40'	0.796	0.049	0.125	0.088	0.014	0.0056	0.572

Table 4. Part 2. Computations associated with depletion within the cloud

Date	I_{ct} ly/min	h	Absorp. by liquid water	$\frac{1}{2}S_A$	$\frac{1}{4}S_{wv}$	A_{wv}	W.V. absorp. of $3/4S_{wv}$	I_{cb} ly/min
May 18	1.224	1000	0.393	0.001	0.005	0.068	0.0012	0.651
May 22	1.121	900	0.384	0.002	0.004	0.065	0.0010	0.609
May 23	0.899	1000	0.474	0.004	0.005	0.069	0.0012	0.401
May 30	1.131	800	0.349	0.005	0.004	0.060	0.0008	0.657
May 31	1.140	1200	0.479	0.012	0.005	0.070	0.0012	0.494
Jun 3	0.591	900	0.550	0.007	0.007	0.104	0.0014	0.195
Jun 13	0.820	700	0.366	0.007	0.008	0.100	0.0016	0.425
Jun 26	0.811	1100	0.531	0.010	0.007	0.100	0.0016	0.284
Jun 28	1.122	1000	0.411	0.007	0.005	0.080	0.0012	0.556
Jun 29	1.206	1100	0.422	0.007	0.004	0.075	0.0009	0.592
Jul 5	1.056	1100	0.451	0.002	0.002	0.055	0.0004	0.518
Jul 6	0.947	1000	0.446	0.004	0.004	0.077	0.0010	0.443
Jul 7	1.098	1100	0.443	0.005	0.005	0.080	0.0012	0.511
Jul 18	0.648	750	0.462	0.008	0.004	0.075	0.0009	0.291
Jul 25	0.730	1000	0.497	0.010	0.006	0.095	0.0015	0.285
Jul 29	0.747	1100	0.536	0.010	0.005	0.087	0.0012	0.270
Jul 30	1.089	1900	0.632	0.008	0.008	0.105	0.0021	0.268
Aug 8	0.517	900	0.575	0.002	0.006	0.095	0.0014	0.165
Aug 11	0.817	1000	0.488	0.002	0.006	0.090	0.0013	0.338
Aug 13	1.068	1300	0.498	0.002	0.006	0.092	0.0015	0.429
Aug 14	1.047	1800	0.632	0.005	0.008	0.105	0.0021	0.260
Aug 15	0.572	1500	0.757	0.010	0.008	0.100	0.0018	0.071

Table 4. Part 3. Computations associated with depletion below the cloud.

Date	I_{cb} ly/min	$\frac{1}{2}S_D$	A_{wv}	$\frac{1}{2}S_A$	$\frac{1}{4}S_{wv}$	W.V. absorp.of 3/4 S_{wv}	I_s ly/min	I_s observed ly/min
18 May	0.651	0.002	0.100	0.005	0.006	0.0015	0.577	0.470
22 May	0.609	0.002	0.080	0.005	0.005	0.0013	0.552	0.410
23 May	0.401	0.002	0.080	0.008	0.005	0.0014	0.362	0.360
30 May	0.657	0.002	0.060	0.010	0.004	0.0008	0.607	0.515
31 May	0.494	0.001	0.025	0.008	0.001	0.0001	0.478	0.430
3 Jun	0.195	0.001	0.073	0.001	0.005	0.0010	0.179	0.240
13 Jun	0.425	0.001	0.075	0.001	0.005	0.0010	0.390	0.410
26 Jun	0.284	0.002	0.090	0.002	0.006	0.0014	0.255	0.290
28 Jun	0.556	0.001	0.075	0.002	0.005	0.0011	0.510	0.560
29 Jun	0.592	0.002	0.090	0.004	0.006	0.0015	0.531	0.540
5 Jul	0.518	0.001	0.070	0.002	0.001	0.0001	0.480	0.450
6 Jul	0.443	0.001	0.065	0.001	0.002	0.0003	0.413	0.320
7 Jul	0.511	0.001	0.060	0.002	0.015	0.0028	0.469	0.330
18 Jul	0.291	0.002	0.090	0.010	0.006	0.0014	0.259	0.240
25 Jul	0.285	0.001	0.065	0.009	0.003	0.006	0.263	0.260
29 Jul	0.270	0.001	0.077	0.010	0.004	0.0009	0.245	0.180
30 Jul	0.268	0.001	0.068	0.010	0.004	0.0009	0.246	0.165
8 Aug	0.165	0.001	0.080	0.002	0.006	0.0011	0.150	0.140
11 Aug	0.338	0.002	0.104	0.004	0.008	0.0020	0.297	0.280
13 Aug	0.429	0.001	0.065	0.001	0.002	0.0005	0.399	0.390
14 Aug	0.260	0.001	0.078	0.001	0.005	0.0012	0.238	0.310
15 Aug	0.071	0.0035	0.120	0.010	0.012	0.0034	0.060	0.060

Table 4. Part 4. Computations concerning cloud albedo.

Date	Z	h feet	h/L	A_F%	liquid water absorp.	A_F applied to liquid water absorp.	$\left\{\frac{1}{2}S_A + \frac{1}{4}S_{wv}\right\}$	A_c%
18 May	32° 19'	1000	10.9	64	0.393	0.251	0.006	25.7
22 May	38° 40'	900	9.8	65	0.384	0.250	0.007	25.7
23 May	49° 20'	1000	10.9	72	0.474	0.341	0.010	35.1
30 May	37° 59'	800	8.7	64	0.349	0.223	0.009	23.2
31 May	36° 40'	1200	13.1	69	0.479	0.331	0.016	34.7
3 Jun	61° 30'	900	9.8	74	0.550	0.407	0.014	42.1
13 Jun	50° 00'	700	7.6	66	0.366	0.242	0.014	25.6
26 Jun	52° 12'	1100	12.0	73	0.531	0.388	0.017	40.5
28 Jun	37° 42'	1000	10.9	67	0.411	0.275	0.012	28.7
29 Jun	32° 12'	1100	12.0	66	0.422	0.279	0.011	29.0
5 Jul	39° 20'	1100	12.0	69	0.451	0.311	0.004	31.5
6 Jul	44° 50'	1000	10.9	70	0.446	0.312	0.008	32.0
7 Jul	36° 40'	1100	12.0	68	0.443	0.301	0.010	31.1
18 Jul	57° 40'	750	8.2	70	0.462	0.323	0.012	33.5
25 Jul	52° 20'	1000	10.9	72	0.497	0.358	0.016	37.4
29 Jul	52° 20'	1100	12.0	73	0.536	0.391	0.015	40.6
30 Jul	37° 00'	1900	20.7	79	0.632	0.499	0.015	51.4
8 Aug	63° 50'	900	9.8	74	0.575	0.426	0.009	43.5
11 Aug	50° 59'	1000	10.9	71	0.488	0.346	0.022	36.8
13 Aug	37° 42'	1300	14.2	72	0.498	0.359	0.007	36.6
14 Aug	41° 00'	1800	19.6	80	0.632	0.506	0.012	51.8
15 Aug	63° 40'	1500	16.4	80	0.757	0.606	0.018	62.4